

Calculation of the free energy of defects in calcium fluoride

J. H. Harding

*Theoretical Physics Division, Atomic Energy Research Establishment,
Harwell, Oxfordshire OX11 0RA, England*

(Received 3 April 1985)

We show how the free energies of defect processes may be calculated directly from a microscopic model. In addition to the calculation of internal energies, we also calculate the vibrational entropy, using a large-crystallite method. Using the results obtained, we comment on the nature and range of validity of the Arrhenius relation. We calculate the ionic conductivity and compare it directly with experiment. Defect volumes are also calculated and compared with the available data.

I. INTRODUCTION

It has long been possible to calculate accurate internal energies of formation for point defects in ionic crystals. Programs such as HADES (Ref. 1) and CASCADE (Ref. 2) have been written to make such calculations a matter of routine provided that the interionic forces within the crystal are known. A review of the assumptions used in such programs is given in the articles in the book edited by Catlow and Mackrodt.³

Progress in methods for calculating entropies of formation has been slower. The high-temperature entropy of formation in the harmonic approximation is given by

$$s_v = -k \ln \left[\frac{\prod_i \omega'_i}{\prod_i \omega_i} \right] \quad (1)$$

(provided that the number of degrees of freedom does not change), where k is Boltzmann's constant and ω'_i, ω_i are the normal-mode frequencies of the defect and perfect crystal, respectively. The subscript v for the entropy denotes a quantity at constant volume, a necessary consequence of the use of the harmonic approximation.

Three ways have been used to calculate entropies with use of (1). The first method, discussed by Harding and Stoneham,⁴ uses a periodically repeating cell containing the defect and surrounding ions and an analogous cell for the perfect lattice. The required frequencies ω'_i, ω_i are assumed to be the phonon modes at zero wave vector. The method relies on the fact that for the large unit cell, the dispersion curve will be folded back onto the Γ point of the reduced Brillouin zone, thus making the phonon modes at this point a reasonable approximation to the required phonon density of states. For a large enough repeating unit this should work. However, the units used up to now^{4,5} have been rather small.

The second method, the Green-function approach, recasts the entropy formula in terms of the Green functions of the perfect lattice and the changes of force constant due to the introduction of the defect. The utility of the method rests on the possibility of confining the changes of force constant to a small region close to the defect. The method is discussed by Jacobs in his article in Ref. 3 and

by Gillan and Jacobs.⁶ However, it has disadvantages when considered as the basis for a general code to calculate the entropies of defects. The calculation of Green functions of sufficient accuracy is a tedious business. Further, as Sangster and Rowell⁷ have pointed out, the Green functions used in most calculations refer to the ionic core displacements as calculated from a static lattice relaxation using the shell model. In such a case the effective force constants should be calculated the same way. This adds further complications.

The third method, the large-crystallite method, is much more suitable for machine computation. This method assumes that the crystal may be divided into two regions, an inner region around the defect where the ions are allowed to vibrate and an outer region where they are held fixed and contribute only to the diagonal elements of the force constant matrix. The required frequencies ω, ω' of Eq. (1) are those of the inner crystallite region for the defect and perfect lattice. The SHEOL⁸ code ("simple harmonic evaluation of lattices") has been written to calculate defect entropies with use of this method.

The availability of computer codes to calculate energies and entropies of defects means that the main problem remaining is the correct specification of the interionic potential. For entropy calculations this is especially important as we require not only an accurate specification of $\phi(r)$ but also of its first and second derivatives. Indeed, if we wish to calculate the entropy as a function of temperature (and therefore of lattice parameter) we require the third derivative as well. The question of how such a potential is found and verified is taken up in a later section of the paper.

Calcium fluoride is a convenient system to use as an illustration of the problem of calculating free energies of defects. There have been a number of previous attempts to calculate the entropy of formation of the anion Frenkel defect,^{4-6,9} and one attempt to calculate the anion diffusion rate.¹⁰ A good deal of experimental data is available on the cation and anion defects and the transport processes. The ionic conductivity has been measured over a range of temperatures by Ure¹¹ and by Jacobs and Ong.¹² Oberschmidt and Lazarus¹³ have also measured the pressure dependence to obtain the defect volumes of formation and migration, extending and, to some extent,

contradicting the earlier work of Lallemand.¹⁴ Data on the cation processes are less easy to come by; however, work has been done by Matzke and Lindner,¹⁵ Berard,¹⁶ and King and Moerman.¹⁷ In this paper we shall confine ourselves to defect processes on the anion sublattice.

We shall first discuss the methods of calculating defect energies and entropies. We shall then turn to the question of the specification of interionic potentials and the calculation of perfect lattice properties before turning to the calculation of defect free energies and their comparison with experiment.

II. THE CALCULATION OF DEFECT PARAMETERS

Methods of calculating defect energies have been frequently discussed before.¹⁻³ Here we merely summarize the main points. The crystal is divided into two regions, an inner region (I) containing the defect and an outer region (II). The ions in region I are iteratively relaxed with use of a fast Newton-Raphson procedure until they reach their positions of zero force. The outer region (II) is treated as a dielectric continuum and the ion positions in this region are obtained by the method of Mott and Littleton.¹⁸ Most calculations assume that the crystal may be described by a simple shell model. In essence, the ions in the crystals are modeled by considering them as massive cores linked to massless shells by a harmonic spring constant. Short-range forces simulating the Pauli repulsion and dispersive attraction terms between the ions act between the shells. Coulomb forces act between cores and shells except for cores and shells on the same ion. Such models give a good representation of the perfect lattice and defect properties. Also, important for our purposes, they give a good representation of the phonon density of states.¹⁹

We now turn to the question of calculating entropies. Using the obvious definition of the defect entropy of formation ΔS_d ,

$$\Delta S_d = S(\text{defect crystal}) - S(\text{perfect crystal}), \quad (2)$$

where the defect crystal contains a single defect, we obtain

$$\Delta S_d = -k \ln \left[\frac{\prod_{i=1}^{3N'} \omega_i'}{\prod_{i=1}^{3N} \omega_i} \right] + 3k(N' - N) \left[1 - \ln \left(\frac{\hbar}{kT} \right) \right], \quad (3)$$

where the primes denote the defective crystal. The final logarithmic term is necessary to correct the dimensions of the first term when $N' \neq N$. This equation defines defect entropies with respect to ions brought in from at rest at infinity or removed to there and so corresponds to the usual definition of internal energies of formation used in codes such as HADES.

It is often useful to express (3) in terms of the determinant of the dynamical matrix. In the harmonic approximation we may write the equations of motion of the ions as

$$(\Phi - \omega^2 \underline{M})\mathbf{u} = \mathbf{0}, \quad (4)$$

where Φ is the force-constant matrix, \underline{M} the mass matrix, and \mathbf{u} the vector of vibrational displacements with respect to the static ion positions. This therefore gives us the product of the vibrational frequencies as

$$\prod_{i=1}^{3N} \omega_i^2 = \frac{\det(\Phi)}{\det(\underline{M})}, \quad (5)$$

and we can therefore rewrite (3) as

$$\Delta S_d = -\frac{1}{2} k \ln \left[\frac{\det(\underline{D}')}{\det(\underline{D})} \right] + 3k(N' - N) \left[1 - \ln \left(\frac{\hbar}{kT m_0^{1/2}} \right) \right], \quad (6)$$

where \underline{D} is the dynamical matrix given by

$$\underline{D} = \underline{M}^{-1/2} \Phi \underline{M}^{1/2}, \quad (7)$$

and m_0 is the atomic unit of mass. Again the last term corrects the dimensions of the first term for $N' \neq N$.

We require the dynamical matrix \underline{D} in terms of the force-constant matrixes for cores and shells. These are given by

$$\Phi_{ll'}^{cc} = \delta_{ll'} \left[\sum_{l''} (\underline{C}_{ll''}^{cc} + \underline{C}_{ll''}^{cs}) \right] - \underline{C}_{ll'}^{cc} + \underline{K}_l \delta_{ll'}, \quad (8a)$$

$$\Phi_{ll'}^{cs} = -\underline{C}_{ll'}^{cs} - \underline{K}_l \delta_{ll'}, \quad (8b)$$

$$\Phi_{ll'}^{sc} = -\underline{C}_{ll'}^{sc} - \underline{K}_l \delta_{ll'}, \quad (8c)$$

$$\Phi_{ll'}^{ss} = \delta_{ll'} \left[\sum_{l''} (\underline{S}_{ll''} + \underline{C}_{ll''}^{ss} + \underline{C}_{ll''}^{sc}) \right] - (\underline{S}_{ll'} + \underline{C}_{ll'}^{ss}) + \underline{K}_l \delta_{ll'}. \quad (8d)$$

The matrices $\underline{C}^{rr'}$ represent the Coulomb forces, the superscripts denoting cores (c) or shells (s). The matrix \underline{S} refers to the short-range forces acting between the shells and the diagonal matrix \underline{K} the harmonic spring constants. The subscripts l, l', l'' denote ions and Cartesian coordinates. The Coulomb sums in (8) are calculated using the Ewald technique as described in Ref. (1) and (6).

We may write the dynamical matrix in terms of these force-constant matrices and obtain

$$\underline{D}_{ll'} = \left[\Phi_{ll'}^{cc} - \sum_{m,n} \Phi_{lm}^{cs} (\Phi^{ss})_{mn}^{-1} \Phi_{nl'}^{sc} \right] / (\underline{M}_l \underline{M}_{l'})^{1/2}, \quad (9)$$

where again the indices denote ion and Cartesian coordinates. We now introduce the basic assumption of the large-crystallite model. We divide the crystal into two regions: an inner region, containing the defect and surrounding ions where the ions are allowed to vibrate, and an outer region, where the ions are held fixed in the positions calculated by the static lattice calculation. Thus the sum over normal modes in (3) or the determinant in (6) is calculated only for ions in the inner region. The ions of the outer region contribute through the diagonal elements of the force-constant matrix, the sums over l'' in Eqs. (8a) and (8d).

In the calculation of charged defects we must apply a correction which arises from the effects of the long-range distortion field. The displacements of the ions far from the defect cause changes in the force constants that fall off as R^{-2} . Since the number of ions in a shell of distance R from the defect grows as R^2 it is clear that the effect of a charged defect on the crystal force constants does not die away with distance. Gillan and Jacobs⁶ have discussed this problem and we apply their correction here. The problem arises not from the defect charge, but from the distortions that it causes. Gillan and Jacobs show that we can obtain the correction we require by considering the entropy of a perfect lattice but with the ionic distortions due to the defect. We require only the term linear in the distortion field and so the ionic displacements are scaled down by a factor λ and the entropy multiplied by the same factor. The correction term ΔS_{corr} is given by

$$\Delta S_{\text{corr}} = \lambda[S'(\lambda) - S(\text{perfect lattice})]. \quad (10)$$

The corrected entropy of formation is given by

$$s_v = \Delta S_d - \Delta S_{\text{corr}}. \quad (11)$$

With this correction, we now have a method for calculating s_v , the entropy of formation at constant volume. It is simple to check the convergence with increasing inner region size and extrapolation to the infinite crystal may readily be done.

In practice, we shall need at least 100 ions for the size of the inner region. The dynamical matrices are large and it is desirable to reduce the problem as much as possible. We therefore block-diagonalize the dynamical matrix \underline{D} by the use of symmetry projection operators. The problem of calculating such operators is well understood and the methods discussed in standard text books. However, the scale of the problem considered here (up to a few hundred ions) makes many of them unsuitable. The one used in SHEOL is an adaptation of the method of Nielsen and Berryman.²⁰ The details of how the operators are constructed are given in a report by Ball and Harding.²¹ Having obtained the required projection operator \underline{U} we may obtain the block diagonal matrix $\underline{\tilde{D}}$ by the standard transformation

$$\underline{\tilde{D}} = \underline{U}^T \underline{D} \underline{U}. \quad (12)$$

It is possible to reduce the double summation over ions and coordinates implied in (12) to a single summation using a result of Crawford.²² Again the details are discussed in Ref. 21.

A SHEOL calculation consists of two parts. The first part is a lattice statics calculation to evaluate the static relaxation of the defect and the internal energy of formation u_v . This is done with the AERE Harwell HADES code. The second part consists of taking the positions of the ions, defining an inner region, and performing three large-crystallite calculations: one on the defective lattice, one on the perfect lattice, and one on the distorted perfect lattice. This gives us ΔS_d and ΔS_{corr} and so enables us to evaluate s_v , the entropy of formation at constant volume.

If we are calculating the vibrational entropy of formation, we should also calculate the vibrational contribution

to the internal energy of formation. We can, however, show that this vanishes in the high-temperature limit.

From standard statistical mechanics the vibration internal energy U of a crystal is given by

$$U = \sum_{i=1}^{3N} \frac{\hbar\omega_i}{\exp(\hbar\omega_i/kT) - 1}. \quad (13)$$

For high temperatures, this reduces to

$$U = 3NkT. \quad (13')$$

Since in the defects we shall be considering the number of ions does not change (although Schottky defects change the number of lattice points in a crystal they do not change the number of ions), the contribution to

$$u_v = U(\text{defect crystal}) - U(\text{perfect crystal}) \quad (14)$$

is zero. If, however, we consider a case where the number of ions in the crystal does change (for example, a non-stoichiometric oxide interacting with oxygen gas), there will be a contribution of

$$u_v = 3(N' - N)kT. \quad (15)$$

A SHEOL calculation thus gives the Helmholtz free energy of formation of an isolated defect,

$$f_v = u_v - Ts_v. \quad (16)$$

Any configurational terms must be calculated separately and any defect-defect interactions (apart from those that can be calculated by Debye-Hückel theory) must be obtained by considering explicit clusters.

Our calculations are calculations at constant volume. However, most experiments are done at constant pressure and so produce the Gibbs free energy of the defect g_p . The various relations between thermodynamic defect parameters have been much discussed in the literature. A convenient collection of the most useful results is to be found in the paper of Catlow *et al.*²³ In particular, we note that to first order in the defect volume v_p ,

$$g_p = f_v. \quad (17)$$

We may thus use SHEOL to calculate the enthalpies and entropies of defects at constant pressure using the standard relations

$$s_p = - \left[\frac{\partial g_p}{\partial T} \right]_p, \quad (18)$$

$$h_p = g_p + Ts_p. \quad (18')$$

This avoids the necessity of calculating the volume of formation as has been done in previous estimates of h_p .

It is instructive to consider these expressions a little more closely. From (17) and (18) and the standard relation

$$\left[\frac{\partial f_v}{\partial T} \right]_p = \left[\frac{\partial f_v}{\partial T} \right]_v + \left[\frac{\partial V}{\partial T} \right]_p \left[\frac{\partial f_v}{\partial V} \right]_T, \quad (19)$$

we obtain

$$s_p = s_v - \left(\frac{\partial V}{\partial T} \right)_p \left(\frac{\partial f_v}{\partial V} \right)_T, \quad (20)$$

assuming that u_v and s_v are functions of the crystal volume only. If we further assume that the entropy s_v at a given temperature can be obtained from the value calculated using the zero-temperature lattice constant, i.e.,

$$s_v(V) = s_v(V_0) + \left(\frac{\partial s_v}{\partial V} \right)_T \delta V, \quad (21a)$$

$$\delta V = T \left(\frac{\partial V}{\partial T} \right)_p, \quad (21b)$$

then we obtain

$$s_p = s_v(V_0) - \left(\frac{\partial V}{\partial T} \right)_p \left[\left(\frac{\partial u_v}{\partial V} \right)_T - 2T \left(\frac{\partial s_v}{\partial V} \right)_T \right]. \quad (22)$$

Note that (21b) assumes that the lattice thermal expansion is constant and that any defect contribution to the thermal expansion is negligible. Since the variation of u_v with volume is usually large, it is most unlikely that $s_v(V_0)$ will be a reasonable approximation to s_p . However, if we perform a similar analysis on the enthalpy we obtain

$$h_p = u_v(V_0) + T^2 \left(\frac{\partial V}{\partial T} \right)_p \left(\frac{\partial s_v}{\partial V} \right)_T. \quad (23)$$

Thus $u_v(V_0)$ will be a good approximation to h_p provided the variation of s_v with volume is small and the lattice thermal expansion is constant. A similar point has been made by Gillan²⁴ and is of considerable importance for two reasons. First, many calculations have been calculations of $u_v(V_0)$ and it has been assumed that this is a reasonable approximation to h_p . Second, most experimental analyses have assumed that h_p and s_p are constant over the temperature range of interest. From (22) and (23) it is clear that this will only be so provided u_v is a linear function of volume and that the variation of s_v with volume is small. This point will be illustrated in more detail later.

If we know u_v and s_v as a function of volume we may also calculate the volume of formation or migration of a defect. The defect volume of formation is defined as

$$v_p = \left(\frac{\partial g_p}{\partial P} \right)_T. \quad (24)$$

It may be shown²⁴ that this may be written as

$$v_p = -\kappa V \left(\frac{\partial f_v}{\partial V} \right)_T, \quad (25)$$

where κ is the isothermal compressibility. This is much more useful for calculation than (24). It has been assumed in the past that the volume variation of the entropy is negligible. As we shall see in Sec. IV, this is a risky assumption to make.

III. THE CALCULATION OF PERFECT-LATTICE PROPERTIES

As noted above, an important part of calculating defect properties is the correct specification of the interionic potential. Gillan and Jacobs used the potential set of Catlow and Norgett,²⁵ except they assumed that the potential extended to third neighbors rather than second neighbors, as assumed by Catlow and Norgett. In a later paper Catlow *et al.*²⁶ point out that the F^- - F^- interaction in their earlier work had an unreasonably large van der Waals term. They fitted a new potential using a splining scheme. However, their scheme enforced continuity only up to the second derivative in the potential. As explained above, for entropy calculations we require continuity in the third derivative. This has been done by changing the splining scheme of Ref. 26 and refitting the parameters. Only small adjustments are required. The details are given in Table I. Figure 1 shows a calculation of the free energy of formation of the anion Frenkel defect for the two potentials. It is clear that the differences are important. This may also be seen from the parameters for the harmonic approximation, u_v^0 and s_v^0 . For the Catlow and Norgett potential $u_v^0 = 2.496$ eV, $s_v^0 = 2.84k$. For the potential used in this work $u_v^0 = 2.71$ eV, $s_v^0 = -1.65k$. Both parameters are significantly different, but clearly the entropy is far more sensitive than the energy. It is therefore of interest to know how adequate the potential of Table I is. We can gain some insight into this by calculating the perfect-lattice properties over a range of temperature and comparing with experiment. We first consider the lattice parameter. The method of calculating this given the interionic potential is given in Ref. 7 and we summarize it here.

As the crystal is expanded there is in general a pressure change. We may divide the pressure change on expanding the crystal from its initial state (of zero-temperature volume V_0 and 0 K) to the volume and temperature required into two parts. We have an elastic pressure change ΔP_{el} due to the effect of lattice expansion on the interion-

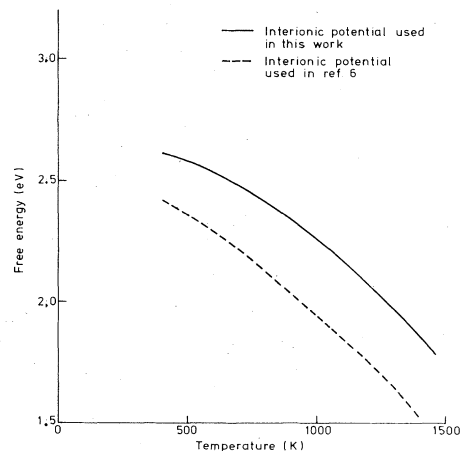


FIG. 1. Effect of interionic potentials on defect parameters (anion Frenkel defect).

TABLE I. Potential parameters for CaF_2 . All short-range interactions are assumed to be zero for $r > 1.5a_0$ (a_0 is the anion-anion distance).

Shell model	
$Y(\text{Ca}^{2+}) = 5.24 e $	$K(\text{Ca}^{2+}) = 390.9 \text{ eV } \text{\AA}^{-2}$
$Y(\text{F}^-) = -2.38 e $	$K(\text{F}^-) = 101.2 \text{ eV } \text{\AA}^{-2}$
Interionic interactions	
$\text{Ca}^{2+}-\text{F}^-$	$\phi(r) = A \exp(-r/\rho)$ $A = 1272.8 \text{ eV } \rho = 0.3002 \text{\AA}$
F^--F^-	$\phi(r) = A \exp(-r/\rho), r < r_a$ = seventh-order polynomial, $r_a < r < r_m$ = fourth-order polynomial, $r_m < r < r_b$ = $-C/r^6, r > r_b$ $A = 1127.2 \text{ eV}, \rho = 0.2753 \text{\AA}, C = 12.0 \text{ eV } \text{\AA}^{-6}$ $r_a = 2.0 \text{\AA}, r_m = 2.726 \text{\AA}, r_b = 3.031 \text{\AA}$ (r_m is the minimum of the potential).

ic forces and a vibrational pressure change ΔP_{vib} due to the effect of lattice expansion on the phonon density of states.

We obtain ΔP_{el} from the definition of the lattice compressibility κ ,

$$\kappa = -\frac{1}{V} \left[\frac{\partial V}{\partial P_{\text{el}}} \right]_T, \quad (26)$$

i.e.,

$$\Delta P_{\text{el}} = - \int_{V_0}^V \frac{dV}{\kappa(V)V}. \quad (27)$$

The dependence of κ upon volume may be calculated using the AERE Harwell PLUTO program.²⁷

The vibrational contribution to the pressure is obtained by differentiating the vibrational contribution to the Helmholtz free energy in the harmonic approximation

$$F_{\text{vib}} = kT \sum_{i=1}^{3N} \ln \left[1 - \exp \left(-\frac{\hbar\omega_i}{kT} \right) \right], \quad (28)$$

$$\Delta P_{\text{vib}} = - \left[\frac{\partial F_{\text{vib}}}{\partial V} \right]_T = \sum_{i=1}^{3N} \frac{\hbar}{\exp(\hbar\omega_i/kT) - 1} \left[\frac{\partial \omega_i}{\partial V} \right]_T. \quad (29)$$

The frequencies and estimates of their derivatives with respect to volume are obtained using a supercell method as discussed by Harding and Stoneham.²⁸ We require the lattice-parameter-versus-temperature relation for one atmosphere. Thus to a very good approximation we require

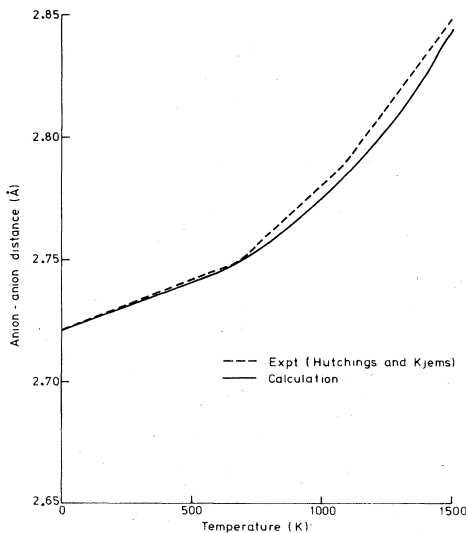


FIG. 2. Lattice parameter for CaF_2 .

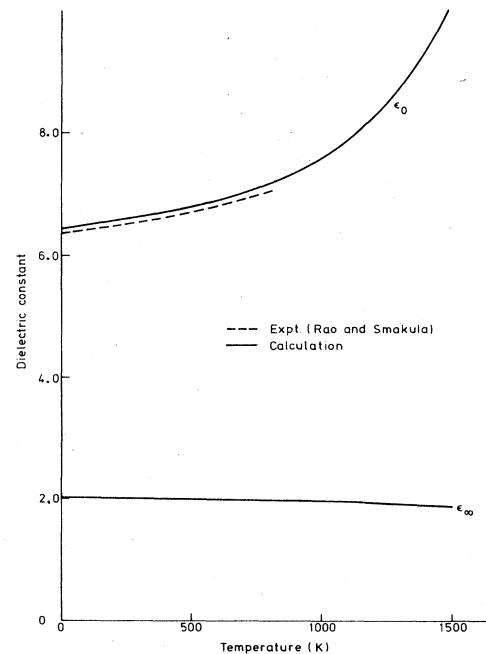


FIG. 3. Dielectric constants for CaF_2 .

$$\Delta P_{\text{el}} + \Delta P_{\text{vib}} = 0. \quad (30)$$

The resulting relation is shown in Fig. 2 compared with the data of Hutchings and Kjems.²⁹ The agreement is excellent. We are now in a position to calculate the other bulk properties using the PLUTO program. The temperature variation of the dielectric constants is shown in Fig. 3 together with the available experimental data of Ref. 30. We may use the temperature variation of ϵ_∞ together with the Brillouin scattering data of Catlow *et al.*³¹ to obtain experimental elastic constants. The shift in wave number, $\Delta\tilde{\nu}_B$, of the Brillouin-scattered light is

$$\Delta\tilde{\nu}_B = \left[\frac{2v_s}{c\lambda_0} \eta \right] \sin(\theta/2), \quad (31)$$

where v_s is the velocity of sound waves causing the scattering, η the refractive index of the crystal, λ_0 the wavelength of the incident light *in vacuo*, c the velocity of light, and θ the scattering angle. The elastic constants are then obtained using the relation

$$c_{ij} = \rho v_s^2. \quad (32)$$

We obtain the elastic constants shown in Fig. 4 where they are compared with those calculated using the PLUTO program. One interesting point is that it is clear from these calculations that the effect of lattice expansion is adequate to explain the variation of c_{11} with temperature, contrary to the suggestion of Catlow *et al.* We may estimate the defect contribution to the compressibility below the fast-ion region as follows. The free energy of the crystal is given by

$$G = G^0 + xg_p - kT \ln W, \quad (33)$$

where the last term is the configurational entropy, x is the concentration of Frenkel defects, and G^0 is the perfect-crystal free energy. Equation (33) assumes that all

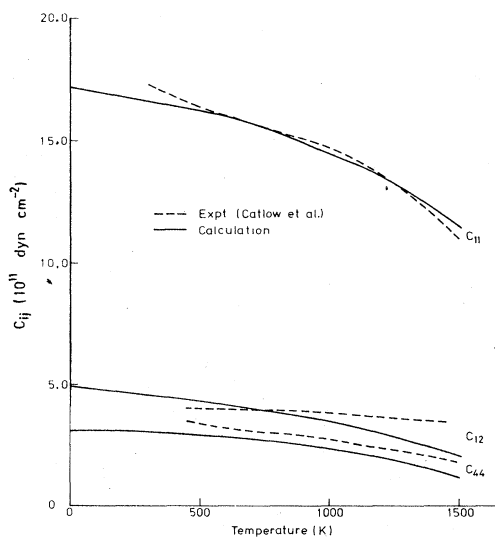


FIG. 4. Elastic constants for CaF_2 .

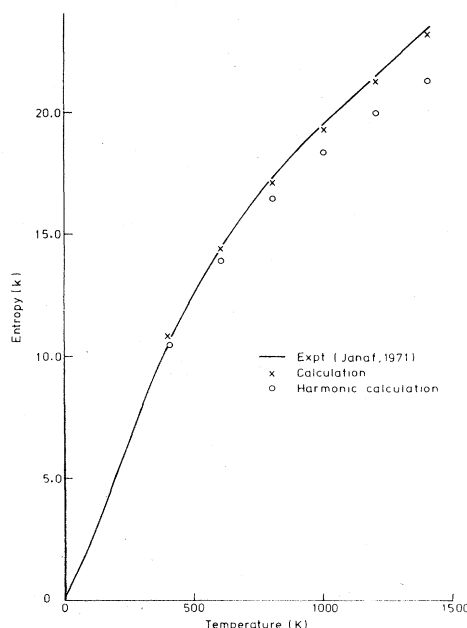


FIG. 5. Entropy of crystalline CaF_2 .

defect-defect interactions may be ignored. Then the crystal volume is given by

$$V = \left[\frac{\partial G}{\partial P} \right]_T = V^0 + xv_p, \quad (34)$$

where V^0 is the perfect-crystal volume and v_p is the defect volume of formation. Thus the compressibility κ of the defect crystal is

$$\kappa = -\frac{1}{V} \left[\frac{\partial V}{\partial P} \right]_T = \kappa^0 + \frac{xv_p^2}{2kTV^0}, \quad (35)$$

assuming that $V^0 \gg xv_p$. We may obtain x knowing g_p from Fig. 6, V^0 from Fig. 2, and v_p from Fig. 9. The correction is of the order of 1% at 1400 K.

The last bulk property of interest is the perfect-lattice entropy. This is shown together with the experimental values³² in Fig. 5. The quasiharmonic approximation is clearly accurate enough to reproduce the experimental results.

The comparison with bulk properties suggests that we have a set of interionic potentials that should give excellent results over a range of temperatures. We now turn to the results of calculation of defect parameters.

IV. DEFECT CALCULATIONS: THE ANION FRENKEL DEFECT

It is convenient to begin by considering the free energy of formation of the anion Frenkel defect. Most attempts to calculate defect parameters in CaF_2 have confined themselves to this. The HADES code may be used to cal-

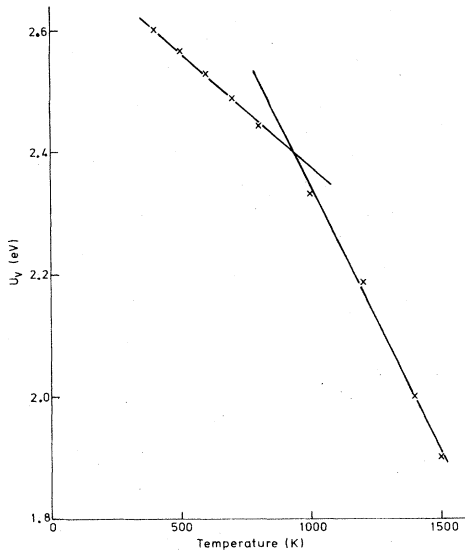


FIG. 6. Anion Frenkel defect: variation of internal energy.

calculate the internal energy of formation u_v as a function of temperature. This is shown in Fig. 6. The entropy as a function of temperature is shown in Fig. 7. An idea of the accuracy of the convergence of the SHEOL calculation is shown in Table II. It is clear that the crystallite sizes of about 100 ions are adequate to give an answer to within $\pm 0.1k$. It is unlikely that the potentials are capable of giving an answer to greater accuracy than that. This is accordingly shown as an error bar on Fig. 7. Also shown are two other calculations of s_v , those of Sahni and Jacobs⁵ using the supercell method and of Jacobs *et al.*³³ using a Green-function method. They clearly differ both from each other and from the current calculation. Two sources of error may be suggested. First, the defect region

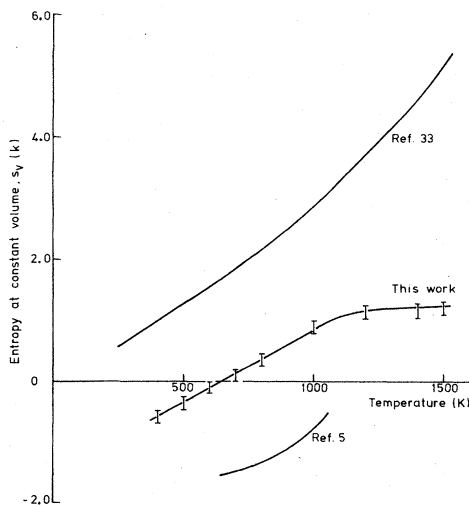


FIG. 7. Variation of s_v with temperature: anion Frenkel defect.

TABLE II. Convergence of entropy calculation for anion Frenkel defect.

Vacancy		Interstitial	
Number of ions in crystallite	$s_v(k)$	Number of ions in crystallite	$s_v(k)$
10	-4.54	15	3.04
34	-4.52	39	3.0
84	-4.42	71	3.03
108	-4.54	127	2.9
160	-4.46	175	2.85
250	-4.46	253	2.83

size for both calculations was small, in the case of the Green-function calculation being only eleven ions. Second, although both calculations used the interionic potentials of Catlow *et al.*,²⁶ neither required continuity in the third derivative of the F^-F^- potential.

Figure 8 shows a plot of the free energy of formation of the defect as a function of temperature. Of particular interest is the point that the calculations fit very well to two straight lines, the changeover point being about 800 K. This corresponds closely to the change in slope in the thermal expansion shown in Fig. 2 and hence to the change of slope in the u_v -versus- T curve in Fig. 6. Table III shows the values of h_p and s_p , the defect parameters at constant pressure, extracted from the calculation. Also shown are the values of the parameters extracted from experiment. It is clear that the values reported are not in substantial disagreement with each other. The differences in value result from the different temperature ranges used. Also, only the lower-range value of h_p corresponds with the standard HADES calculation of u_v^0 .

Since u_v and s_v are functions of volume only, and only functions of temperature through the variation of the lattice parameter, we can consider Figs. 6 and 7 as showing

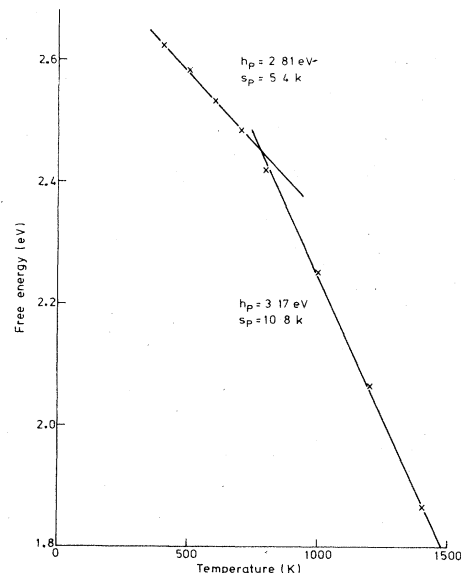


FIG. 8. Calcium fluoride (anion Frenkel).

TABLE III. Anion Frenkel defect parameters.

Temperature range (K)	h_p (eV)	$s_p(k)$	Reference
500–1000	2.71	5.5	12
300–1200	2.74	13.4	35
910–1200	2.82	13.5	11
870–1100	3.0 ± 0.16		13
400–800	2.81	5.4	calculation
800–1500	3.17	10.8	

the variation of u_v and s_v with volume. Figure 6 shows that the plot of u_v versus temperature does analyze into two straight lines. If we consider the variation of s_v with volume the situation is more complex. At high temperatures (large volumes) the variation is negligible. Even at lower temperatures the effect is not large. The slope is about $7.2 \times 10^{-5} \text{ eV K}^{-1} \text{ \AA}^{-3}$, which gives a correction to $u_v(V_0)$ of about 0.06 eV to obtain h_p at 700 K from Eq. (23). The experimental error in fitting defect parameters is frequently as large as this.

However, the volume variation of the entropy does affect the volume of formation. This is shown in Fig. 9 both including and ignoring the entropy term. The calculations give good agreement with the data of Oberschmidt and Lazarus,¹³ but not with those of Lallemand.¹⁴ This is due to Lallemand's low value for the activation volume. We note also that these calculations support the original analysis of Oberschmidt and Lazarus and not the revised analysis of Fontanella *et al.*,³⁴ who based their revised estimate on the assumption that there is a considerable interstitial contribution to the activation volume in the temperature range 800–1000 K. If we compare the calculation with the earlier work of Gillan,²⁴ we see that the volumes of formation calculated here at high temperatures are higher than his. This is partly because of his

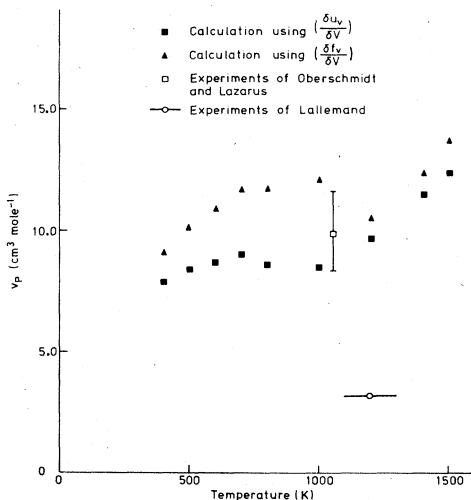


FIG. 9. Anion Frenkel volume of formation.

neglect of the entropy term and partly because he underestimates the lattice expansion and increase of lattice compressibility.

V. MIGRATION PROCESS

We calculate free energies of migration using Vineyard's³⁸ analysis of the simple equation for defect jump rates,

$$\Gamma = \tilde{\nu} \exp \left[-\frac{u_m}{kT} \right]. \quad (36)$$

In this expression Γ is the jump rate, u_m the energy of migration, and $\tilde{\nu}$ an effective frequency association with the vibration of the diffusing ion in the direction of the saddle point. Vineyard's analysis gives a precise meaning to an expression for these quantities. Since experimental results are usually presented using an enthalpy and entropy of migration rather than an effective frequency and an energy, it is convenient to use the alternative formulation of Flynn.³⁹ We write the jump rate Γ as

$$\Gamma = \nu_0 \exp \left[-\frac{f_m}{kT} \right], \quad (37)$$

$$f_m = u_m + kT \left[\sum_{j=1}^{3N} \ln \left(\frac{h\nu'_j}{kT} \right) - \sum_{j=1}^{3N} \ln \left(\frac{h\nu_j}{kT} \right) \right], \quad (38)$$

$$\nu'_{3N} = \nu_0, \quad (39)$$

where the primes refer to frequencies at the saddle point and u_m is the internal energy of migration. Although (37) bears a superficial resemblance to (36), it should be noted that in (37) the frequency ν_0 is arbitrary. It is common to use either the Debye frequency or an optic mode. The fre-

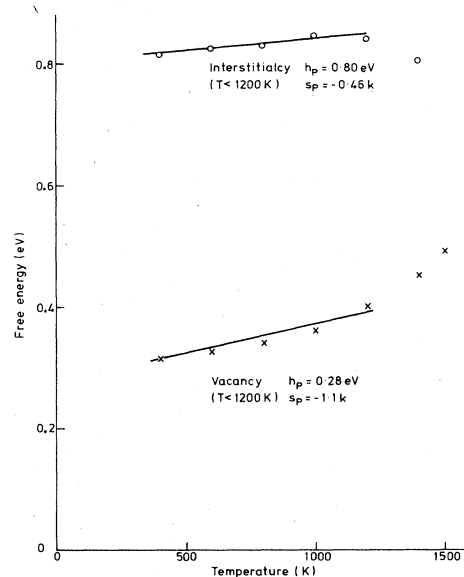
FIG. 10. Migration mechanisms in CaF_2 .

TABLE IV. Anion migration parameters.

Vacancy	h_p (eV)	$s_p(k)$	Reference
(free)	0.33–0.55	1.1–1.9 ^a	12
	0.55		36
	0.51	1.23 ^c (0.59 ^a)	35
	0.52		13
	0.26	–1	calculation
Interstitialcy (free)	0.78	5.3–7.3 ^a	12
	1.0		36
	0.83	–1.4 ^a	calculation
Vacancy (bound to Na ⁺)	0.504	1.24 ^b	37
	0.51	0.56 ^b	calculation ($T < 250$ K)
	0.49	0.0 ^b	calculation ($250 < T < 1000$ K)
Interstitialcy (bound to Y ³⁺)	0.42	0.81 ^b	42
	0.56	0.81 ^b	calculation

^a ν_0 taken to be $1.4 \times 10^{13} \text{ sec}^{-1}$ (optic mode).

^b ν_0 taken to be $8 \times 10^{12} \text{ sec}^{-1}$.

^c ν_0 taken to be $7.14 \times 10^{12} \text{ sec}^{-1}$ (Raman mode).

quency used is noted in the tables where necessary. The SHEOL program may be used to evaluate the frequencies in (38) and so produce an entropy of migration. Calculated free energies of migration for the vacancy and noncollinear interstitialcy process are shown in Fig. 10 and compared with the available experimental data in Table IV (we assume that the interstitial saddle point is where the two F⁻ interstitials are equidistant from the F⁻ vacancy). As can be seen, the calculations predict that the intrinsic conductivity should be completely dominated by the vacancy mechanism, even at high temperatures. The upward curvature of the free energy for both processes is due to the high value chosen for the arbitrary frequency ν_0 .

It is of interest to try and compare these calculations directly with the experimental data. For this we require free energies of association. For convenience we take the M^{3+} impurity assumed by Jacobs and Ong to be Y³⁺. We may then calculate the free energy of association of the interstitial with Y³⁺ and that of the vacancy with Na⁺. Suitable shell-model parameters were chosen from

TABLE V. Shell-model parameters for Na⁺ and Y³⁺.

Shell model	
$Y(Y^{3+}) = 7.53 e $	$K(Y^{3+}) = 252.4 \text{ eV } \text{Å}^{-2}$
$Y(Na^+) = 2.216 e $	$K(Na^+) = 125.2 \text{ eV } \text{Å}^{-2}$
Interionic interactions: $\phi(r) = A \exp(-r/\rho)$	
$Y^{3+}-F^-$	$A = 2298.5 \text{ eV}, \rho = 0.2917 \text{ Å}$
Na^+-F^-	$A = 1189.8 \text{ eV}, \rho = 0.2677 \text{ Å}$

TABLE VI. Association parameters for anion conductivity.

	h_p (eV)	$s_p(k)$	Reference
Vacancy bound to Na ⁺	–0.71	–1.54	12
	–0.85	–2.78	calculation ($T < 1000$ K)
Interstitial bound to M ³⁺	–0.65	0.0 to –0.8	12
	–0.6	0.0	calculation ($T < 700$ K)
	–0.81	–3.4	calculation ($T > 700$ K)

the literature^{40,41} and are shown in Table V. Comparison with the fitted data of Jacobs and Ong is shown in Table VI, and the free energies are plotted in Fig. 11.

We may now calculate the conductivity using the formulas set out by Jacobs and Ong. Figure 12(a) compares the calculated conductivity for sodium-doped CaF₂ with the data of Jacobs and Ong. There is one parameter used in the fitting, the concentration of Na⁺. This is higher than the fitted value quoted by Jacobs and Ong, 2.2×10^{-5} as opposed to 7.8×10^{-6} . The calculation of the “intrinsic” conductivity is shown in Fig. 12(b). Here agreement is poor. The reason is that the calculated free energy of interstitial migration has little dependence on temperature compared to that obtained from the fitting process. Thus the assumption of an M³⁺ impurity cannot bring the calculation into agreement with experiment. It is unfortunate that the data on M³⁺ doped CaF₂ are too poor to give a value for the migration entropy of an interstitial. It is worth noting that the assumption of an O²⁻ impurity would allow much better agreement with experiment, and this impurity is known to be a common contaminant of CaF₂.

It is possible to calculate migration volumes for the vacancy and interstitialcy mechanisms using Eq. (25). These

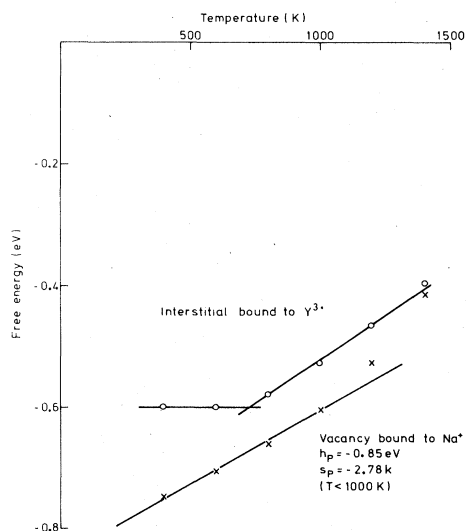


FIG. 11. Association free energies.

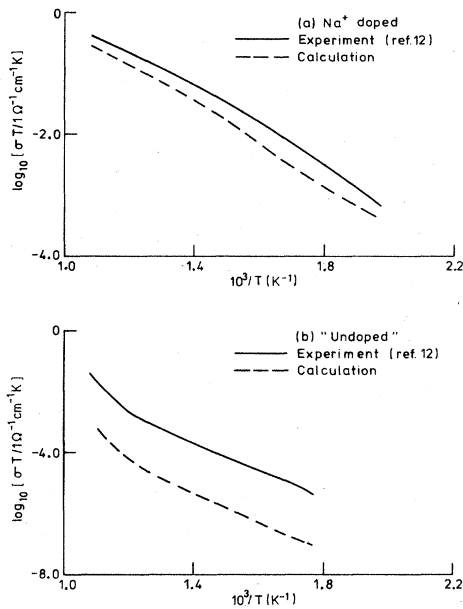


FIG. 12. Conductivity of calcium fluoride.

are shown in Fig. 13. Thus it is possible to calculate the activation volumes and compare the results directly with experiment without having to rely on an analysis to decompose the activation volume into a formation volume and a migration volume. Figure 14 shows the activation volume for the vacancy mechanism compared with the experimental data of Oberschmidt and Lazarus¹³ and of Lallemand.¹⁴ There is, as with the formation volumes, a significant difference between the results including and ignoring the volume variation of the entropy. Figure 15 shows the activation volume for vacancy and interstitialcy. They are very similar. In particular, the results of

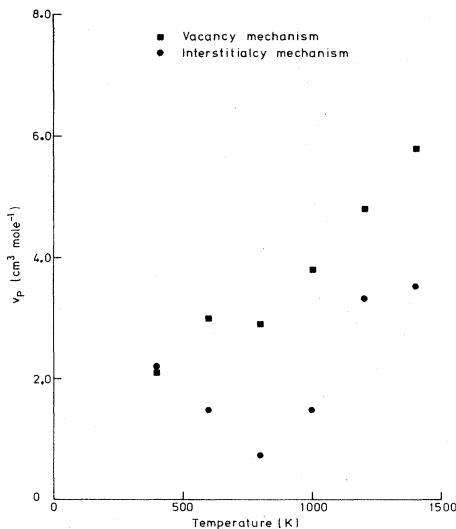
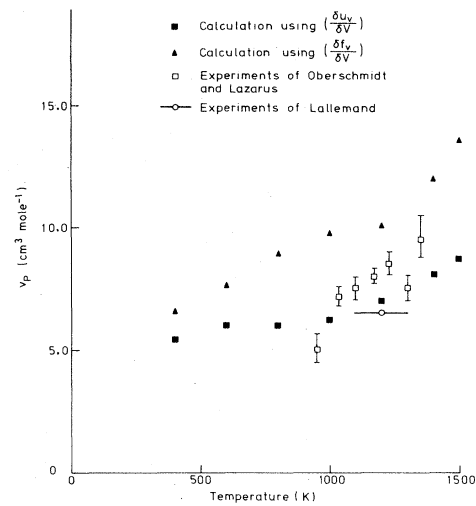
FIG. 13. Migration volumes for CaF₂ (theory).

FIG. 14. Activation volume for vacancy migration.

Figs. 13 and 15 taken together do not support the reanalysis of Fontanella *et al.*,³⁴ which suggests that the migration volume of the interstitialcy is about $7 \text{ cm}^3 \text{ mol}^{-1}$ and that there is a substantial interstitial contribution to the conductivity. The comparison of experiment with the calculated activation volumes suggests that the experimental results are compatible with a mixture of vacancy and interstitialcy conduction pathways, but that the interstitialcy migration volume is similar to or smaller than the vacancy migration volume.

We may also obtain the migration volumes of the bound vacancy and interstitial and compare with the values derived from the pressure dependence of the complex impedance by Fontanella *et al.*³⁴ This is shown in Table VII. The agreement is very reasonable, especially for the interstitial. It has frequently been assumed and indeed may be derived from the dynamical diffusion

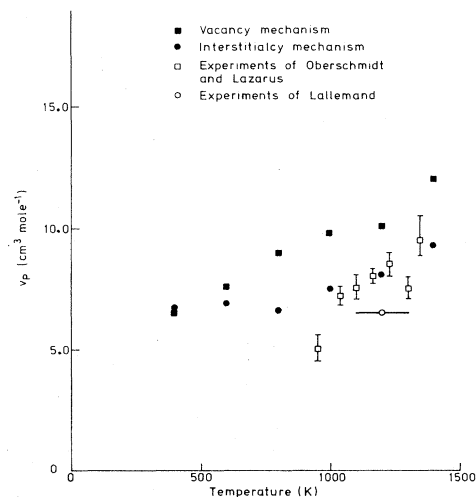


FIG. 15. Activation volume for anion migration.

TABLE VII. Comparison of migration volumes of bound defects at 200 K.

Defect	v_p (experiment) ($\text{cm}^3 \text{mol}^{-1}$)	v_p (calculation) ($\text{cm}^3 \text{mol}^{-1}$)
Vacancy	1.74	0.79
Interstitial	2.9	2.88

theory of Flynn³⁹ that the migration volume is directly proportional to the free energy of migration. It was this assumption that allowed Fontanella *et al.* to estimate the migration volume of the free interstitial. Table VIII shows the free energies and volumes of migration for the four defect processes considered in this paper. There is no evidence of such a linear relationship in this case.

VI. CONCLUSIONS

We have shown that a general method exists for calculating entropies of defect processes in ionic crystals, and that the results of such calculations can be of use in understanding a wide range of defect processes, including the routine calculation of defect volumes. The major problem remaining is the validation of interionic potentials. The comparison shown here suggests that the potentials used give a good representation of the crystal properties over a wide range of temperatures. However, in many systems at high temperatures it will be necessary to address the problem of calculating temperature-dependent corrections to the potential. Work on this problem is currently in progress.

It has frequently been suggested (e.g., Ref. 43) that a useful approximation to the free energy of a defect is given by

$$g_p = CB\Omega, \quad (40)$$

where B is the bulk modulus, Ω a "volume of dilatation," and C an arbitrary constant characteristic of the defect. It is usually assumed that Ω is the atomic volume of the atom involved in the defect. Here we take it to be the molar volume of the crystal. The ratio between this and the atomic volume is a function of the crystal structure and can be absorbed into the constant C . It is of interest to see how well this simple formula performs. Figure 16 shows the calculation of the anion Frenkel free energy compared with that obtained by (40). The constant C is

TABLE VIII. Comparison of calculated volumes and free energies of migration at 800 K.

Mechanism	v_p ($\text{cm}^3 \text{mol}^{-1}$)	g_m (eV)
Bound interstitialcy	0.0	0.51
Free interstitialcy	0.8	0.84
Bound vacancy	1.7	0.49
Free vacancy	2.9	0.34

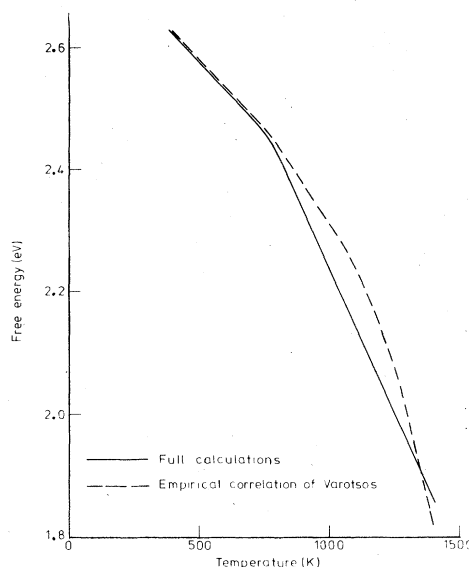


FIG. 16. Comparison of full calculation and Varotsos correlation for the anion Frenkel defect.

obtained by assuming that Eq. (40) gives the correct free energy at 600 K. As can be seen, the formula predicts the qualitative behavior of the free energy. This is not surprising. From Eq. (35) we can see that Eq. (40) states that the free energy is proportional to $(\partial P/\partial V)_T$. Thus Eq. (40) states that the free energy of formation of a defect scales as the stiffness of the crystal lattice. Equation (40) has been applied to free energies of migration. This will work provided that the effect of the change in internal energy dominates the change in the effective frequency $\tilde{\nu}$ of Eq. (36). The variation of these with temperature is shown in Table IX for the vacancy mechanism.

What this suggests is that Eq. (40) has some value as an empirical correlation. However, such an equation has no predictive value. Given the defect free energy for one process one cannot use it to try and predict the free energy for another one. This is because all the detailed physics of the process of defect formation is in the arbitrary constant. Such correlations, therefore, although they may have their uses, must not be confused with serious attempts to calculate defect parameters from a microscopic model.

TABLE IX. Comparison of the internal energy of migration and the effective frequency $\tilde{\nu}$ [see Eq. (36)] (calculation).

T (K)	u_v (eV)	$\tilde{\nu}$ (THz)
400	0.27	3.28
600	0.26	3.62
800	0.24	3.28
1000	0.22	2.46
1200	0.19	1.84
1400	0.14	1.08

- ¹M. J. Norgett, AERE Harwell Report No. R.7650, 1974 (unpublished).
- ²M. Leslie, Daresbury Laboratory Report No. DL/SCI/TM31T, 1982 (unpublished).
- ³*Computer Simulation of Solids*, Volume 166 of *Lecture Notes in Physics*, edited by C. R. A. Catlow and W. C. Mackrodt (Springer, New York, 1982).
- ⁴J. H. Harding and A. M. Stoneham, *Philos. Mag.* **B 43**, 705 (1981).
- ⁵V. C. Sahni and P. W. M. Jacobs, *Philos. Mag.* **A 46**, 817 (1982).
- ⁶M. J. Gillan and P. W. M. Jacobs, *Phys. Rev. B* **28**, 759 (1983).
- ⁷M. J. L. Sangster and D. K. Rowell, *J. Phys. C* **15**, 5153 (1982).
- ⁸J. H. Harding, *Physica B* (to be published).
- ⁹T. M. Haridasan, J. Govindarajan, M. A. Nerenberg, and P. W. M. Jacobs, *Phys. Rev. B* **20**, 3481 (1979).
- ¹⁰J. H. Harding, in *The Physics of Superionic Conductors and Electrode Materials*, edited by J. W. Perram (Plenum, New York, 1983).
- ¹¹R. W. Ure, *J. Chem. Phys.* **26**, 1363 (1957).
- ¹²P. W. M. Jacobs and S. H. Ong, *J. Phys. (Paris) Colloq.* **37**, C7-331 (1976).
- ¹³J. Oberschmidt and D. Lazarus, *Phys. Rev. B* **21**, 5823 (1980).
- ¹⁴M. Lallemand, Ph.D. thesis, University of Paris, 1972.
- ¹⁵Hj Matzke and R. Lindner, *Z. Naturforsch.* **19a**, 1178 (1984).
- ¹⁶M. F. Berard, *J. Am. Ceram. Soc.* **54**, 144 (1971).
- ¹⁷A. D. King and J. Moerman, *Phys. Status Solidi* **22**, 455 (1974).
- ¹⁸N. F. Mott and M. J. Littleton, *Trans. Faraday Soc.* **34**, 485 (1938).
- ¹⁹W. Cochran, *Crit. Rev. Solid State Sci.* **2**, 1 (1971).
- ²⁰J. R. Nielsen and L. H. Berryman, *J. Chem. Phys.* **17**, 659 (1949).
- ²¹R. Ball and J. H. Harding, AERE Harwell Report No. M.3294, 1983 (unpublished).
- ²²B. Crawford, *J. Chem. Phys.* **21**, 1108 (1953).
- ²³C. R. A. Catlow, J. Corish, P. W. M. Jacobs, and A. B. Lidiard, *J. Phys. C* **14**, L121 (1981).
- ²⁴M. J. Gillan *Philos. Mag.* **A 43**, 301 (1981).
- ²⁵C. R. A. Catlow and M. J. Norgett, *J. Phys. C* **6**, 1325 (1973).
- ²⁶C. R. A. Catlow, M. J. Norgett, and T. A. Ross, *J. Phys. C* **10**, 1627 (1977).
- ²⁷C. R. A. Catlow and M. J. Norgett, AERE Harwell Report No. R.2763, 1976 (unpublished).
- ²⁸J. H. Harding and A. M. Stoneham, *J. Phys. C* **17**, 1179 (1984).
- ²⁹M. T. Hutchings and J. Kjems (private communication).
- ³⁰K. V. Rao and A. Smakula, *J. Appl. Phys.* **37**, 319 (1965).
- ³¹C. R. A. Catlow, J. D. Comins, F. A. Germano, R. T. Harley, and W. Hayes, *J. Phys. C* **11**, 3197 (1978).
- ³²*JANAF Thermochemical Tables*, 2nd ed., edited by D. R. Stull and H. Prophet (U.S. GPO, Washington, D.C., 1971).
- ³³P. W. M. Jacobs, M. A. H. Nerenberg, J. Govindarajan, and T. M. Haridasan, *J. Phys. C* **15**, 4245 (1982).
- ³⁴J. J. Fontanella, M. C. Wintersgill, A. V. Chadwick, R. Saghafian, and C. G. Andeen, *J. Phys. C* **14**, 2451 (1981).
- ³⁵W. Bollmann and H. Henniger, *Phys. Status Solidi A* **11**, 367 (1972).
- ³⁶W. Bollmann, P. Görlich, W. Hank, and M. Mothes, *Phys. Status Solidi A* **2**, 157 (1970).
- ³⁷J. J. Fontanella, A. V. Chadwick, V. M. Carr, M. C. Wintersgill, and C. G. Andeen, *J. Phys. C* **13**, 3457 (1980).
- ³⁸G. H. Vineyard, *J. Phys. Chem. Solids* **3**, 121 (1957).
- ³⁹C. P. Flynn, *Point Defects and Diffusion* (Oxford University Press, Oxford, 1972), Chap. 7.
- ⁴⁰P. W. M. Jacobs (private communication).
- ⁴¹C. R. A. Catlow, K. M. Diller, and M. J. Norgett, *J. Phys. C* **10**, 1395 (1977).
- ⁴²C. Andeen, D. Link, and J. J. Fontanella, *Phys. Rev. B* **16**, 3762 (1977).
- ⁴³P. Varotsos and K. Alexopoulos, *J. Phys. Chem. Solids* **38**, 997 (1977).